A synthetic test of residual statics

Joseph H. Higginbotham*
Z-Terra Inc.

Summary

In the early 1970's Taner, Koehler and Alhilali introduced the near surface time anomaly correction method that the industry now refers to as *surface consistent residual statics* or often just *residual statics*. Recall that in those days *digital computers* were just beginning to be used for processing seismic data and that computer memory was measured in units of kilobytes instead of gigabytes. Having a megabyte of memory was not even in the dreams of most geophysicists of that time. This meant that modeling near surface time anomalies due to anomalous near surface velocity structures was not practical. The usefulness of the residual statics method had to be inferred from its ability to improve normal moveout velocity analysis. Even now in the third decade of the 21st century, the small grid spacing required to do finite difference modeling of fine velocity structures in 3D is challenging. However it is fairly easy to do such acoustic modeling of a 2D seismic line. The objective here is to do 2D acoustic modeling of near surface velocity anomalies that give rise to timing anomalies and use this synthetic survey to test the original algorithm of Taner et al. The result is that the method, while not a perfect solution, is found to perform surprisingly well.

Introduction

The literature on residual statics is now vast and varied. Here we return to the original surface consistent method of Tanner et al. (1974) and test it against an overthrust model with significant near surface anomalous velocity structure creating anomalous time shifts.

Consider the velocity model shown in Figure 1. The air layer, above the modeled earth surface, is chosen thick enough to avoid any contamination of synthetic shots by reflection from the model surface. A low velocity weathering layer with velocity of 1000 m/s below the earth surface has filled the *eroaded l*ayer of material of velocity 1600 m/s. Beneath this are dipping layers in the basin and approximately flat layers well behind the thrust fault. The basin has a flat surface but the surface behind the thrust fault has some strong elevation variations. This allows testing residual statics over: (1) a flat surface with mildly dipping reflectors in the basin, (2) over flat reflectors with surface topography well behind the thrust and (3) over complex structure and complex topography at the thrust fault.

Method

A pseudo spectral modeling code implementing a 10th order time derivative was used to model 800 2D shot records spaced 50 meters apart over the velocity model shown in Figure 1. Grid spacing used in modeling was 10 meters horizontally and 2 meters vertically. Split spread shot records were generated with a maximum offset of 4.7 km. Simulated detectors were spaced 50 meters to produce 25 meter CMP spacing.

Figure 2A shows a CMP gather in the basin after shifting to a flat datum 150 m above the basin floor. After this datum shift the surface consistent residual statics algorithm will not distinguish statics due to

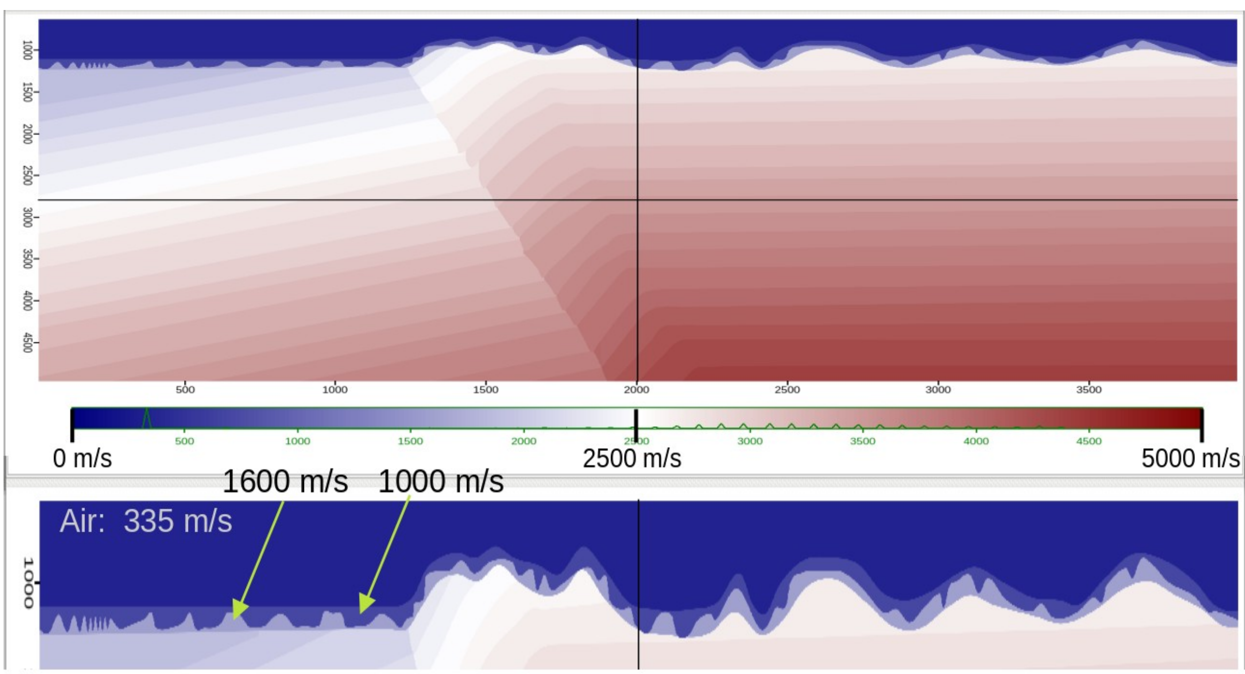

Figure 1*: The 2D over-thrust velocity model with complex velocity variation in the near surface layer intended for testing the residual statics method. On the left are dipping layers over a flat surface. On the right are approximately flat layers over complex topography. At the fault there is a combination of dipping layers and complex topography. Vertical grid spacing is 2 m and horizontal spacing is 10 m.*

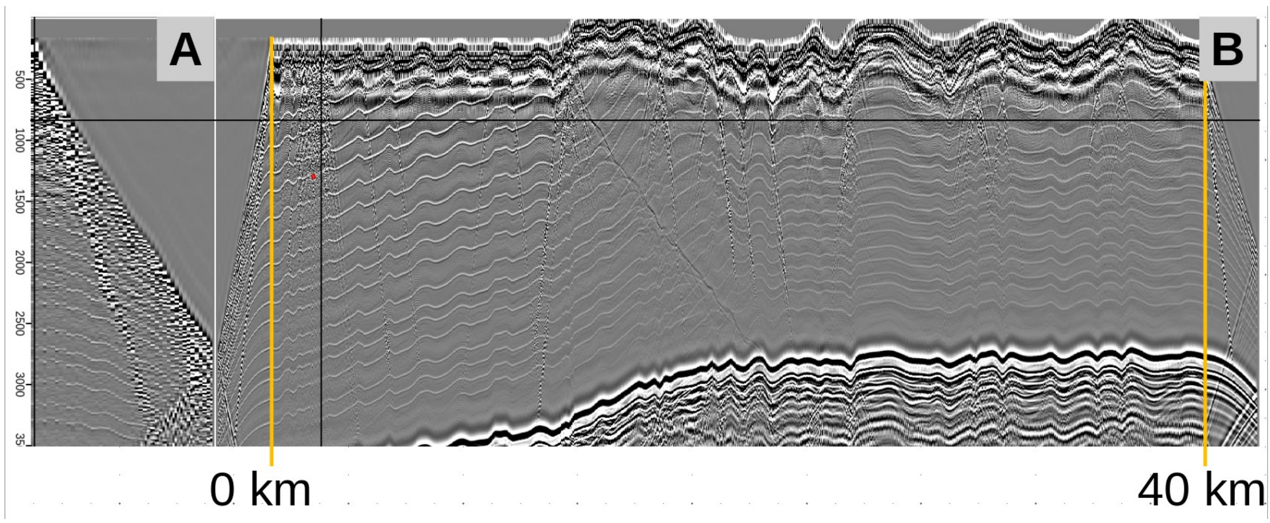

*Figure 2: **A** - CMP gather on the left, **B** - The near offset section on the right after shifting to a flat datum 150 m above the flat basin.*

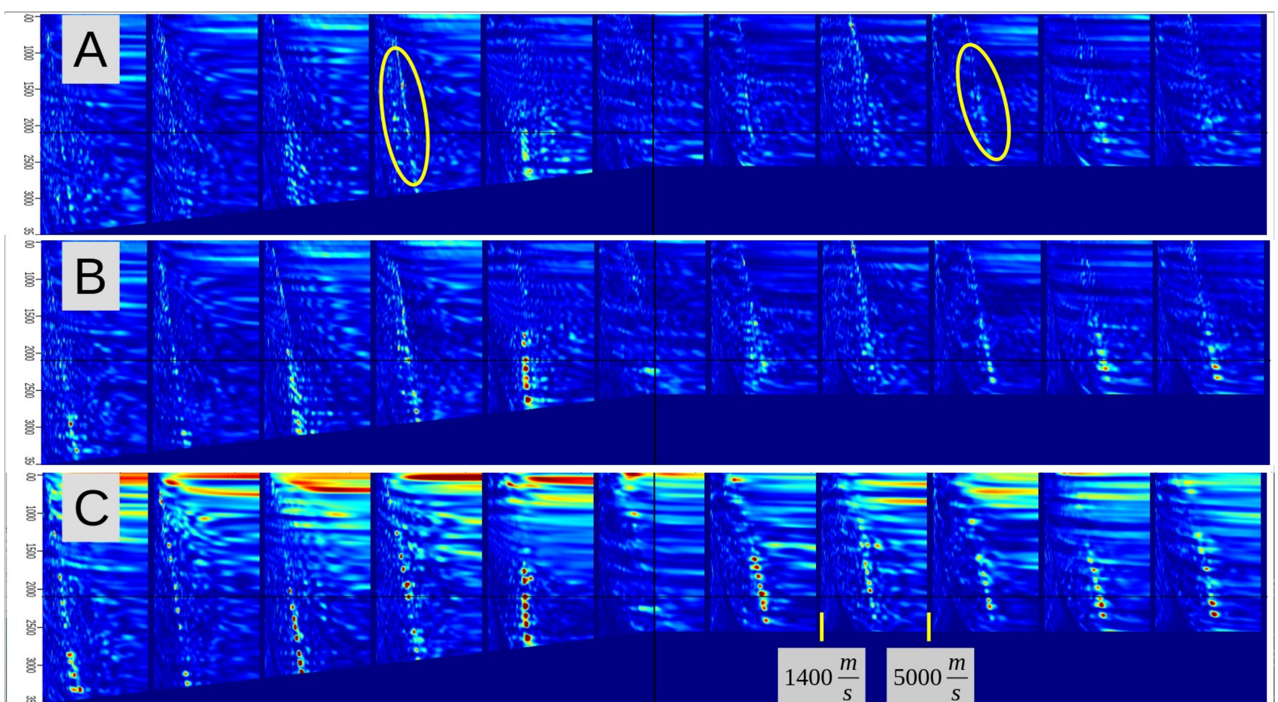

*Figure 3: Uniformly spaced Velocity-Semblance after shifting to flat datum, max semblance clipped at 0.2: **A** - before statics; **B** - after statics corrections were applied to CMPs on flat datum, **C** – statics corrections applied following NMO, then inverse NMO before computing semblance.*

subsurface velocity anomalies from statics caused by datuming errors. The method will seek to correct for both.

Stacking Velocity Analysis

Figure 3A shows some velocity-semblance plots for CMP gathers uniformly distributed over the simulated 2D line. The non-hyperbolic nature of the reflection events in the CMP gathers leads to very noisy semblance plots with only a few showing hints of velocity structure that can be trusted. Only three moveout velocity functions were picked. There are 1600 total CMP locations. Two of the velocity functions were located at CMP numbers: 49 and 449 in the basin. The third was at CMP 1449 well behind the thrust fault near the end of the line of CMPs. This velocity function was duplicated and translated to CMP 900 just behind the thrust fault. This NMO velocity, Vnmo-1, was linearly interpolated between these picked velocity functions. Fortunately there is a residual NMO term in the surface consistent residual statics algorithm so it can tolerate some error in NMO. The residual statics program was then run in a time window between 1500 ms and 2300 ms, the resulting statics were transferred to the headers of the input CMPs and applied. Then another velocity-semblance computation was performed to produce the results shown in Figure 3B. The semblance plots in Figure 3B are much improved and are more easily interpreted. Velocity functions were picked at CMP’s 49, 199, 349, 499, 699, 899, 1199, 1449 and 1599 to be used to build NMO velocity Vnmo-2 for subsequent passes of residual statics.

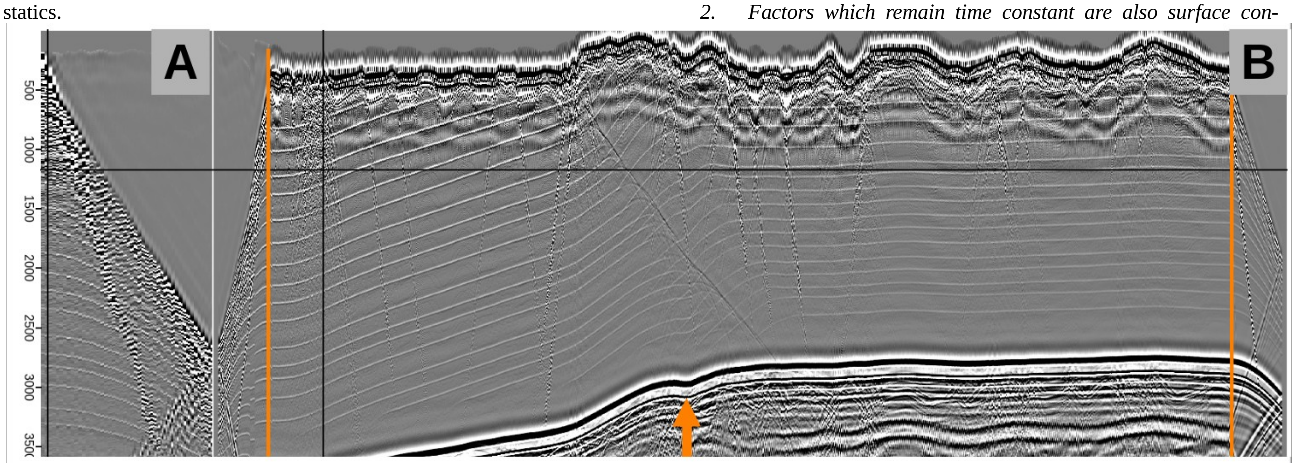

Figure 4: Gather, A, and near offset section, B, after four passes of residual statics.

NMO and statics application do not commute

Figure 3C is a velocity-semblance plot produced by applying the residual statics to moved out gathers and then applying inverse NMO before doing the velocity-semblance analysis. These semblance plots are much easier to interpret. This is because NMO does not commute with the *application of static corrections*. These semblance plots look very good in the basin but behind the thrust fault they look best inside the time window used in the statics computation.

This issue with NMO not commuting with statics application means that even if the residual statics that are computed will remove anomalous shifts from moved out gathers on the first pass, those statics applied to the input gathers *before* NMO may not completely remove the anomalous shifts. This explains the difference between the quality of the semblance in Figure 3B and Figure 3C.

Ideally we want NMO and *application of residual statics* to commute. To accomplish this the following steps were applied repeatedly:

1. apply NMO to input CMP gathers,
2. perform residual statics computation,
3. apply statics to input CMP gathers,
4. examine CMP gathers for obvious anomalous shifts,
5. if anomalous shifts are found return to step 1 with statics corrected CMP gathers to compute further residual statics.

On the third pass of surface consistent residual statics using Vnmo-2 for each pass (fourth pass of residual statics if the pass using Vnmo-1 is included), the result shown in Figure 4 was reached – compare with Figure 2.

Continued application of residual statics beyond the fourth pass had no significant effect on the reflection events in front of or behind the thrust fault. However, each subsequent pass caused the static *dimple* indicated by the orange arrow in Figure 4, to grow – distorting all reflection events above.

Residual statics assumptions

Taner and Koehler (1981) list the following assumptions that were made to implement surface consistent applications.

1. *Factors due to effects at or near the surface are constant throughout the recording time; these include source response, source coupling, attenuation in the near-surface layers, geophone sensitivity, and geophone coupling.*
2. *Factors which remain time constant are also surface consistent. This means that the effects associated with a particular surface position remain constant regardless of the wave path. For example, source strength will affect all of the traces recorded from that source. Similarly, the geophone coupling effect remains the same for all traces recorded at a particular receiver station from various source positions.*
3. *Common-depth-point (CDP) gathering is assumed to be valid. By this we mean that all traces at a particular CDP gather position contain essentially the same sub-surface information.*
4. *The corrections for spherical divergence, normal move-out, and field statics have been applied. We do this to eliminate most of the amplitude and arrival time corrections, so that within a time window all traces of a CDP gather satisfy the previous assumption.*

For this synthetic test these assumptions hold, or hold approximately, except at the overthrust fault where the third assumption should be violated because of lateral velocity variations and steep dip. This may suggest a cause for the divergence of the dimple (Figure 4) with continued application of the algorithm.

The residual statics implementation used here

Taner et. al. (1974) indicates four effects that contribute to a static time shift: (1) receiver statics, (2) source statics, (3) CMP statics, and (4) a residual NMO static proportional to the square of the offset. These statics are all computed separately in general. However the residual NMO static is not applied. Taner et. al. also argue that to have an optimal match with the stack of input CMP gathers, the CMP statics must be zero.

The implementation of the algorithm used here provides the option to computes a CMP static and to apply or not apply that static. As used here the CMP static was computed but not applied. Separate static shifts were

A synthetic test of residual statics

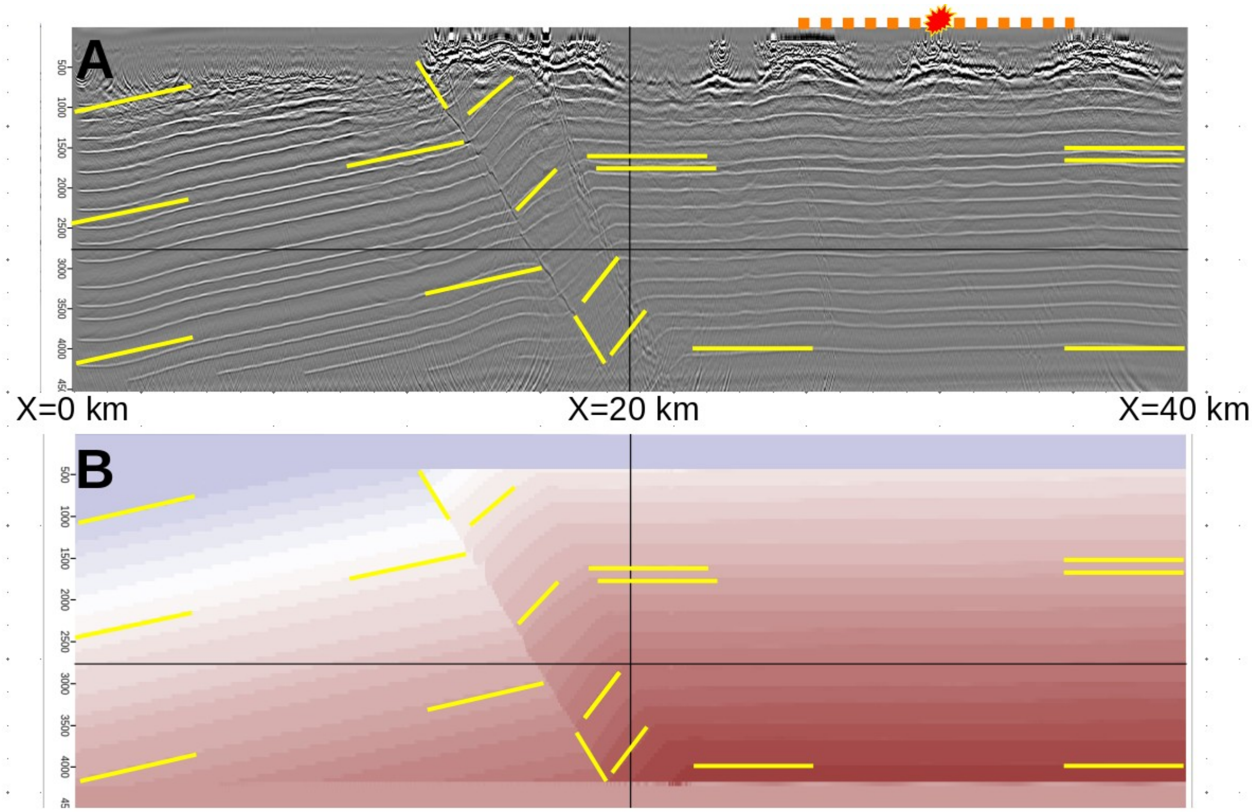

Figure 5: The poststack (of figure 4 data) depth migration following residual NMO, ***A****, was done with the velocity field* ***B*** *where the velocity structure of the topography has been replaced with a constant velocity of 2000 m/s. The yellow lines help to identify differences between the imaged structure and the velocity model. The relative size of the split-spread shot records is shown above* ***A****. There were 189 simulated detectors.*

computed for source and receiver positions.

The static shifts involved in the computation were computed by first defining a *pilot trace* for each CMP gather. The pilot trace was formed by stacking the input CMP gathers. Cross-correlation provides a static time shift. However, after statics were computed they were applied, a new pilot trace computed, and new static shifts found for another iteration of the computation. In the cases shown here there were four such iterations of pilot trace computation for each pass of residual statics.

The normal equations for the least-mean-square error were solved by iteration.

Noise

The affect of random noise was also studied. The algorithm performed well in areas away from the thrust fault even when the signal to noise ratio was ¼ and reflection events could not be identified on plotted CMP gathers. In this case the noise level of the stack approaching the thrust fault was too high to evaluate algorithm performance with certainty. There was a faint indication that the method was failing as the thrust fault was approached on the mountainous side of the line. This was also true and obvious for the case of signal to noise ratio ½ . However in both cases the failure was the introduction of a long wavelength static with wavelength approximately twice the length of the detector pattern for a shot record. Even for the case of signal to noise ½ the thrust fault was identifiable and reasonably well positioned. At signal to noise of 1.0 the results were comparable to the solution with no added random noise.

Datum and Imaging

Various floating datums were tested but the best result was produced by using the flat datum. Figure 5A shows the result of doing a post-stack depth migration of the stack of Figure 4 data followed by residual NMO. Figure 5B shows the velocity field used for imaging. Essentially all near surface velocity anomalies and topography have been replaced in the velocity model with the 2000 m/s replacement velocity used to go to the flat datum prior to computing and applying residual statics. The result, while definitely not perfect, is surprisingly good. A pre-stack depth imaging method might produce much improved results.

Conclusions

For residual statics to work at all the cross-correlation in the chosen time window must be able to compute a static shift that defines the error to be found and removed.

Going to a flat datum before residual statics computation produced the best results. The algorithm computed a static time shift that compensated for: (1) the near surface velocity anomalies, (2) errors associated with datuming. The compensation was approximately equivalent to replacing the zone of velocity anomaly and topography with a constant layer filled with the replacement velocity as indicated by the imaging in Figure 5.

This synthetic test indicates that residual statics leaves behind only long wavelength statics to be addressed with other methods.

A synthetic test of residual statics

References

Taner, M. Turhan, F. Koehler and A Alhilali, (1974) Estimation and correction of near-surface time anomalies, Geophysics, Vol. 39, No 4

Taner, M. Turhan, Fulton Koehler, (1981) Surface consistent corrections, Geophysics, Vol 46, No 1